

Towards Resilient Transportation: A Conditional Transformer for Accident-Informed Traffic Forecasting

Hongjun Wang
The University of Tokyo
Tokyo, Japan

Jiawei Yong
Toyota Motor Corporation
Tokyo, Japan

Jiawei Wang
The University of Tokyo
Tokyo, Japan

Shintaro Fukushima
Toyota Motor Corporation
Tokyo, Japan

Renhe Jiang*
jiangrh@csis.u-tokyo.ac.jp
The University of Tokyo
Tokyo, Japan

Abstract

Traffic prediction remains a key challenge in spatio-temporal data mining, despite progress in deep learning. Accurate forecasting is hindered by the complex influence of external factors such as traffic accidents and regulations, often overlooked by existing models due to limited data integration. To address these limitations, we present two enriched traffic datasets from Tokyo and California, incorporating traffic accident and regulation data. Leveraging these datasets, we propose ConFormer (Conditional Transformer), a novel framework that integrates graph propagation with guided normalization layer. This design dynamically adjusts spatial and temporal node relationships based on historical patterns, enhancing predictive accuracy. Our model surpasses the state-of-the-art STAEFormer in both predictive performance and efficiency, achieving lower computational costs and reduced parameter demands. Extensive evaluations demonstrate that ConFormer consistently outperforms mainstream spatio-temporal baselines across multiple metrics, underscoring its potential to advance traffic prediction research. *The code is released in <https://github.com/Dreamzz5/ConFormer>.*

CCS Concepts

• Information systems → Spatial-temporal systems; • Computing methodologies → Artificial intelligence.

Keywords

Spatio-temporal forecasting, Traffic accident, Urban computing

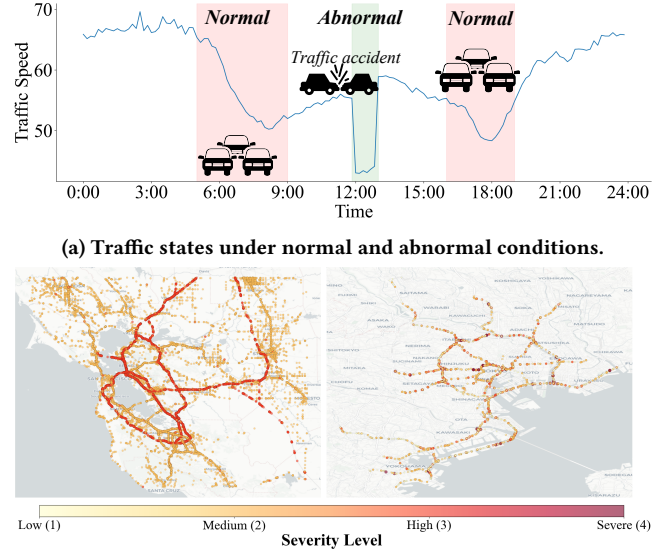
ACM Reference Format:

Hongjun Wang, Jiawei Yong, Jiawei Wang, Shintaro Fukushima, and Renhe Jiang. 2026. Towards Resilient Transportation: A Conditional Transformer for Accident-Informed Traffic Forecasting. In *Proceedings of the 32nd ACM SIGKDD Conference on Knowledge Discovery and Data Mining V.1 (KDD '26)*, August 09–13, 2026, Jeju Island, Republic of Korea. ACM, New York, NY, USA, 11 pages. <https://doi.org/10.1145/3770854.3780312>

*Corresponding author.



This work is licensed under a Creative Commons Attribution 4.0 International License. *KDD '26, Jeju Island, Republic of Korea*
© 2026 Copyright held by the owner/author(s).
ACM ISBN 979-8-4007-2258-5/2026/08
<https://doi.org/10.1145/3770854.3780312>



(b) Accidents by severity level in the California and Tokyo regions.

Figure 1: Illustration of our motivation: enhancing traffic forecasting towards resilient transportation.

1 Introduction

Traffic forecasting remains a key challenge in intelligent transportation systems, supporting route planning, emergency response, and urban traffic management. While deep learning has made major progress in recent years, predicting traffic conditions still faces a critical problem: existing methods work well for regular patterns but struggle when traffic accidents disrupt normal flow. As shown in Figure 1a, traffic systems follow predictable patterns during normal conditions (like rush hours), but traffic accidents cause sudden speed drops and complex changes that current spatiotemporal methods cannot handle well. Studies show that traffic incidents greatly reduce prediction accuracy, with highway accidents contributing significantly to overall travel delays [11, 22]. Real-world data shows that accidents can increase travel times by 37-43% compared to normal conditions [17, 18].

Traffic systems show a basic conflict between predictable and unpredictable behavior. Normal traffic follows known time patterns, with rush hour congestion well captured by models like DCRNN [35]. However, accidents create complex disturbances that

spread through connected road networks in nonlinear ways [62, 67], producing severe disruptions beyond what current spatiotemporal methods can model. This reveals two main problems in current approaches: (1) **Limited accident data coverage**. Most traffic datasets lack detailed incident information, offering only basic flow data, which prevents systematic study of how accidents and regulations affect traffic patterns [5]; (2) **Inadequacies in accident modeling**. Current approaches ignore incident factors entirely, failing to account for how accidents change spatial relationships, time dependencies, and data patterns during disrupted conditions [48, 62].

To address these fundamental limitations, first, we create two comprehensive datasets integrating detailed incident information with traditional flow measurements. Our Tokyo dataset covers 1,843 highway segments with accident and regulatory data from JARTIC [26], while our California dataset encompasses Bay Area (2,352 sensors) and San Diego (716 sensors) with comprehensive accident classifications from the US Accidents database [43]. As demonstrated in Figure 1b, accident distributions exhibit significant geographic variation in density and severity patterns across the Bay Area and Tokyo regions.

Building upon recent advances in conditional modeling [46, 65], we propose ConFormer, a novel conditional Transformer architecture for incident-aware traffic prediction. The core innovation lies in our Guided Layer Normalization (GLN) mechanism, which replaces static normalization parameters with dynamic affine transformations conditioned on prevailing traffic conditions [45]. This enables adaptive modulation of internal feature distributions during incident scenarios where conventional normalization proves inadequate. ConFormer integrates GLN with graph propagation mechanisms that diffuse incident information across traffic networks, capturing complex spatiotemporal correlations when localized incidents propagate through interconnected road segments [31]. Despite sophisticated conditioning mechanisms, ConFormer maintains computational efficiency with reduced parameters and overhead compared to STAEFormer [37], achieving superior predictive accuracy while preserving scalability for real-world deployment. We make the following contributions:

- **ConFormer**, a conditional Transformer employing guided layer normalization to adaptively capture spatiotemporal dynamics with incident awareness;
- **Two large-scale datasets**: Tokyo highways with accident and regulatory data, and California highways with comprehensive accident annotations;
- **State-of-the-art performance** surpassing STAEFormer across normal and incident scenarios while maintaining superior computational efficiency with fewer parameters and lower overhead.

2 Related Works

Spatiotemporal forecasting has garnered significant attention due to its critical importance in various real-world applications. Traditional approaches such as ARIMA [44], VAR [50], k -NN [12], and SVM [51] often struggle to effectively capture the complex dependencies inherent in spatiotemporal data. Deep learning has led to substantial advancements in spatiotemporal forecasting. Recurrent Neural Networks, including LSTMs [41, 42] and GRUs [10], have shown considerable success in modeling temporal dynamics.

However, these models frequently fall short in capturing spatial dependencies, which are essential for accurate predictions in networked urban systems. To address this shortcoming, the integration of Graph Convolutional Networks (GCNs) with temporal models has been proposed, resulting in notable improvements in spatiotemporal forecasting. Prominent examples include STGCN [66] and DCRNN [35], which have laid the groundwork for further advancements in the field [4, 7, 61, 62]. Additionally, a variety of innovative methods have been developed [28, 33, 47, 56, 63], including meta-parameter learning approaches [15], normalization techniques [14], large-scale forecasting methods [23], expert frameworks [52], and curriculum learning strategies [54]. Time series transformers [9, 58] have also been employed to capture spatiotemporal correlations [25, 27, 37, 69] and manage long sequences [39, 59, 70, 71]. Recent advances include masked pre-training strategies for spatiotemporal forecasting [19] and efficient transformer architectures [53]. Although traffic accidents significantly influence traffic propagation, the extent and mechanisms of these effects remain insufficiently explored. While some studies have addressed multi-incident co-prediction [57] and traffic accident risk prediction [68, 72], existing approaches often treat accidents as external factors rather than integrated components of the forecasting model. *To address this gap, our study proposes a novel conditional transformer architecture, which integrates guided normalization layers to dynamically adjust node spatial relationships and temporal correlations in response to traffic accidents, providing a more resilient and powerful traffic forecasting technique.*

3 PROBLEM STATEMENT

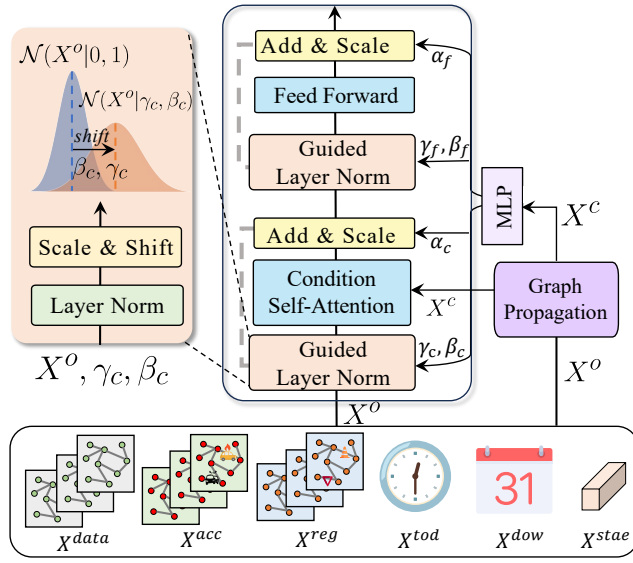
The traffic network is modeled as a graph $G = (\mathcal{V}, \mathcal{E}, \mathcal{A})$, where \mathcal{V} represents N nodes, \mathcal{E} denotes edges, and $\mathcal{A} \in \mathbb{R}^{N \times N}$ encodes node relationships. Traffic states over past T time steps observed at time t are expressed as $X_t \in \mathbb{R}^{T \times N \times D}$, where D is the feature dimension (e.g., flow or speed). In this study, dynamic traffic conditions such as traffic accident or regulation are incorporated as guided features. Our target is to predict the traffic state for the future T' time steps $\hat{Y}_t \in \mathbb{R}^{T' \times N \times 1}$, where \hat{Y}_t denotes the predicted traffic states, thus our problem is defined as $[X_t; \mathcal{A}] \xrightarrow{q(\cdot)} (\beta, \gamma, \alpha)$ and $[X_t; \beta, \gamma, \alpha] \xrightarrow{f(\cdot)} \hat{Y}_t$, where $q(\cdot)$ computes global factors β, γ, α to guide the prediction model $f(\cdot)$.

4 Methodology

The overall architecture of our proposed ConFormer is illustrated as Figure 2. We expand its details in the following sections.

4.1 Spatiotemporal Condition Propagation

The data embedding layer transforms input observations X_t into a high-dimensional representation $X^{data} \in \mathbb{R}^{T \times N \times D_{data}}$ via a fully connected layer, where D_{data} is the embedding dimension. To incorporate domain knowledge, we design spatiotemporal embeddings that capture both network structure and traffic periodicity. Following the concatenation order in our final embedding, we first incorporate traffic event indicators $X^{acc} \in \mathbb{R}^{T \times N \times D_{acc}}$, $X^{reg} \in \mathbb{R}^{T \times N \times D_{reg}}$ for accidents and regulations respectively. To model traffic periodicity patterns, we introduce weekly and daily embeddings $\omega(t) \rightarrow X^{dow} \in \mathbb{R}^{T \times N \times D_{dow}}$, $\tau(t) \rightarrow X^{tod} \in \mathbb{R}^{T \times N \times D_{tod}}$, where



$\omega(t)$ maps to week indices (1-7) and $\tau(t)$ to time-interval indices (e.g., 1-288 for 5-minute intervals in a day). The temporal embeddings X^{dow}, X^{tod} are constructed by concatenating embeddings across all time steps T . Moreover, we incorporate spatiotemporal adaptive embedding $X^{stae} \in \mathbb{R}^{T \times N \times D_{stae}}$ [37] and concatenate all the embeddings together as follows:

where \parallel denotes the concatenation operation.

Graph Propagation. To model the accident propagation effect, we leverage the idea of graph propagation from GCN [31], which operate over a graph \mathcal{G} . Given a graph signal $X \in \mathbf{R}^{|\mathcal{V}| \times D}$, where D is the number of node features, a typical K -hop graph convolutional layer is formulated as $GCN_{\mathcal{G}}(X; W, \theta) = \sigma \left(\sum_{k=0}^K \theta_k \mathcal{L}^k X \right) W$, where $\mathcal{L} \in [0, 1]^{|\mathcal{V}| \times |\mathcal{V}|}$ is the graph Laplacian of the adjacency matrix \mathcal{A} that controls information propagation between nodes; $\theta \in \mathbf{R}^K$ weights contributions from different hops; $W \in \mathbf{R}^{N \times D'}$ (D' is the output feature dimension) mixes feature dimensions; and σ denotes the activation function. In our work, to model the condition propagation effect (i.e., the accident impact), we simplify the GCN by applying only the graph propagation and omitting the feature mixing with W on the input embedding X^o , as follows:

X^c can be regarded as a contextual condition representation that incorporates the propagation effect.

The spatiotemporal Transformer architecture has shown superior performance in traffic forecasting [37]; therefore, we adopt it as the backbone of our model. Given the traffic input embedding X^o , the query, key, and value for the self-attention mechanism are computed as follows:

where W_Q, W_K, W_V are learnable parameters. Then, for spatial dependencies, at each time step t , we compute the spatial attention scores as: $A_t^{(Sp)} = \frac{Q_{t,:,:} (K_{t,:,:})^\top}{\sqrt{d'}}$ where $Q_{t,:,:}, K_{t,:,:}, V_{t,:,:} \in \mathbb{R}^{N \times d'}$ are the query, key, and value matrices for the spatial dimension. The output of the spatial self-attention is then obtained as: $X^{(Sp)} = \text{softmax}(A_t^{(Sp)}) V_{t,:,:}$. Similarly, for temporal dependencies, we compute the temporal attention scores for each node n as: $A_n^{(Te)} = \frac{Q_{:,n,:} (K_{:,n,:})^\top}{\sqrt{d'}}$ where $Q_{:,n,:}, K_{:,n,:}, V_{:,n,:} \in \mathbb{R}^{T \times d'}$ are the query, key, and value matrices for the temporal dimension. The output of the temporal self-attention is then obtained as: $X^{(Te)} = \text{softmax}(A_n^{(Te)}) V_{:,n,:}$. Finally, an MLP is employed to fuse $X^{(Sp)}$ and $X^{(Te)}$ into a unified spatiotemporal representation:

Although the backbone is capable of capturing spatiotemporal dependencies, real-world traffic states are inherently dynamic and complex. Factors such as traffic accidents, local regulations, and sudden demand fluctuations introduce substantial variations that are challenging to model. To address this challenge, we propose *Guided Layer Normalization (GLN)* to substitute the classic LayerNorm [3], which adapts the normalization process using dynamic, condition-dependent parameters derived from the contextual condition representation.

Guided Layer Normalization. LayerNorm [3] is widely used to stabilize the training of deep neural networks by normalizing inputs across features. Given an input X^o , it is computed as: $X^o = \gamma \frac{X^o - \mu}{\sigma} + \beta$, where μ and σ are the mean and standard deviation of the elements in X^o , and γ and β are learnable but fixed parameters shared across all inputs. Instead, we propose to learn dynamic affine transformation factors γ, β from the condition representation X^c and guide the normalization as follows:

With GLN, the vanilla self-attention (applied along spatial/temporal axis) can be reformulated as follows:

where $\mathbf{Q}' = \gamma \cdot \frac{\mathbf{Q} - \mu_{\mathbf{Q}}}{\sigma} + \beta$ and $\mathbf{K}' = \gamma \cdot \frac{\mathbf{K} - \mu_{\mathbf{K}}}{\sigma} + \beta$. The proof of this reformulation is provided in Appendix. Based on this formulation, we can derive the following interpretations:

- **For γ (scaling factor):**
 - **Higher γ :** Increases sensitivity to abrupt changes in traffic patterns, enabling rapid adaptation to accidents or anomalies.

- **Lower γ** : Suppresses the influence of local fluctuations, promoting stability under regular traffic conditions.
- **For β (shifting factor)**:
 - **Higher β** : Emphasizes node-specific features, strengthening local feature representation in response to accidents.
 - **Lower β** : Preserves global coherence, facilitating smoother information exchange across nodes.

γ and β serve distinct yet complementary roles in guiding and adapting spatiotemporal modeling with Transformer. Their interplay enables the Transformer to balance global patterns with localized variations for robust performance across diverse scenarios.

Condition Self-Attention. Given the input embedding X^o and the contextual condition representation X^c , GLN is applied to get the normalized input representation $X^{(GLN)}$ through Eq. (5) that adapts to the current traffic context. Building upon this, we extend the vanilla self-attention in Eq. (3) to a *conditional* variant that incorporates both normalized input features and contextual condition information. Specifically, we override Eq. (3) as follows:

$$\begin{aligned} Q &= X^{(GLN)} W_Q, \\ K &= (X^{(GLN)} \parallel X^c) W_K, \\ V &= (X^{(GLN)} \parallel X^c) W_V. \end{aligned} \quad (7)$$

The subsequent spatial/temporal attention computations are identical to those in Eq. (4), allowing seamless integration of our conditional self-attention into the spatiotemporal Transformer backbone.

Conditional Residual Connections. Given the contextual condition representation X^c , we propose learning a modulation factor α via an MLP, $\alpha = \text{MLP}(X^c)$, to scale each module's output through the residual connections. The design of this mechanism is informed by insights from [20], where zero-initialization is leveraged to enhance the stability and efficiency of large-scale training processes. This approach has demonstrated significant benefits when applied to complex datasets like San Diego and Bay Area [38]. From a conceptual perspective, this mechanism resonates with the principles of curriculum learning [6]. By prioritizing the learning of fundamental, intrinsic features in the initial stages, the model progressively integrates additional contextual signals, which are typically noisier. This staged learning process improves optimization during training by enabling the model to focus on mastering essential patterns before adapting to more complex or variable information.

Building on the above components, we now present the whole workflow of our proposed ConFormer as follows:

- **Conditional Branch.** The conditional branch refines input features X^o using graph structure \mathcal{A} through GraphPropagation, producing conditional features X^c . The MLP then outputs the conditional factors:

$$X^c = \text{GraphPropagation}(X^o, \mathcal{A}), \quad (8)$$

$$[\gamma_c, \beta_c, \alpha_c] = \text{MLP}_c(X^c). \quad (9)$$

Here, β_c and γ_c parameterize the mean and variance in GLN, while α_c scales residual connections to enhance feature interactions. These factors adaptively influence the transformer branch through context-aware attention and normalization.

- **Transformer Branch.** The transformer branch incorporates the conditional factors as follows:

$$X^{(GLN)} = \text{GLN}(X^o, \gamma_c, \beta_c), \quad (10)$$

$$X^{(Att)} = \text{ConditionAttention}(X^{(GLN)}, X^c), \quad (11)$$

$$X^{(Res)} = X^o + \alpha_c X^{(Att)}. \quad (12)$$

The ConditionAttention module enables dynamic adaptation of feature interactions, while the scaled residual connection α_c ensures information continuity and stability.

- **Feedforward Layer.** The feedforward module further processes the features using a secondary set of conditional factors $[\gamma_f, \beta_f, \alpha_f]$, also derived from X^c via an MLP as follows:

$$[\gamma_f, \beta_f, \alpha_f] = \text{MLP}_f(X^c).$$

These factors are applied to the normalized features through another GLN layer as follows:

$$X'^{(GLN)} = \text{GLN}(X^{(Res)}, \gamma_f, \beta_f), \quad (13)$$

$$X^{(FF)} = \text{FeedForward}(X'^{(GLN)}), \quad (14)$$

$$\hat{Y}_t = X^{(Res)} + \alpha_f X^{(FF)}. \quad (15)$$

The residual connections, scaled by α_f , maintain model stability while facilitating deeper feature transformation.

4.3 Computational Complexity

We partition the computational complexity of ConFormer into three primary components and calculate the FLOPs for each as follows:

- **Graph Propagation.** Graph propagation leverages the Chebyshev polynomial approximation with a computational complexity of $O(K|\mathcal{E}|D)$, where K denotes the order of the polynomial, $|\mathcal{E}|$ represents the number of edges, and D is the number of channels. This complexity primarily arises from the approximation of the graph Laplacian operator.
- **Condition Self-Attention.** The complexity of spatiotemporal condition self-attention is $O(TN^2D + NT^2D)$, where N is the number of spatial nodes and T is the temporal length.
- **GLN.** The generation of γ , β , and α for layer normalization and residual connections incurs a computational cost of NTD^2 .

Given that ConFormer is largely controlled by conditions, a single attention layer suffices to achieve superior performance. Therefore, the total FLOPs of ConFormer can be computed as:

$$\text{FLOPs(ConFormer)} = K|\mathcal{E}|D + (TN^2D + NT^2D) + NTD^2.$$

Table 1: Summary of Our Developed Datasets.

Dataset	Tokyo	San Diego	Bay Area
Start Time	2021/10/1	2019/1/1	2019/1/1
End Time	2021/12/31	2019/12/31	2019/12/31
Time Interval	10 minutes	15 minutes	15 minutes
#Spatial Units	1,843 road links	716 sensors	2,352 sensors
Traffic Source	MegaCRN [28]	LargeST [38]	LargeST [38]
Accident Source	JARTIC ¹	US Accidents [43]	US Accidents [43]
Regulation	✓	✗	✗
Accident	✓	✓	✓

Table 2: Performance comparison with improvements over the best baseline. All models incorporate incident data, for example, GWNet and AGCRN expand features, while STAEFormer and STID use binary embeddings. **Bold purple indicates the best results (ConFormer), **brown underlined** indicates the second-best results (best baseline).**

DATA	METHOD	PARAM	10 MIN			30 MIN			60 MIN			AVERAGE		
			MAE	RMSE	MAPE	MAE	RMSE	MAPE	MAE	RMSE	MAPE	MAE	RMSE	MAPE
TOKYO ($N = 1,843$) (ACCIDENT ✓) (REGULATION ✓)	LSTM [24]	98K	7.00	11.10	31.95%	7.74	12.40	36.45%	8.65	13.81	41.81%	7.68	12.24	35.88%
	AGCRN [4]	771K	5.99	9.48	25.71%	6.64	10.73	29.81%	6.99	11.39	32.13%	6.64	10.53	29.88%
	STGCN [66]	1.1M	6.09	9.70	24.84%	6.91	11.09	30.24%	8.41	12.80	32.90%	7.24	11.20	29.99%
	GWNET [62]	333K	5.91	9.40	25.22%	6.59	10.64	29.78%	6.89	11.17	31.71%	6.56	10.40	29.90%
	STGODE [16]	769K	6.08	9.57	26.51%	6.74	10.75	30.29%	7.15	11.48	32.91%	6.79	10.64	30.87%
	STID [48]	576K	6.08	9.56	25.87%	6.85	10.90	31.25%	7.46	11.32	32.31%	6.60	10.51	29.81%
	DSTAGNN [32]	17.8M	5.90	9.39	24.53%	6.68	10.87	29.93%	7.11	11.66	32.56%	6.67	10.64	29.34%
	DGCRN [34]	333K	5.86	9.36	24.80%	6.49	<u>10.54</u>	<u>29.23%</u>	<u>6.81</u>	<u>11.11</u>	<u>31.39%</u>	<u>6.49</u>	<u>10.34</u>	29.47%
	D ² STGNN [49]	426K	<u>5.85</u>	<u>9.35</u>	<u>24.52%</u>	<u>6.49</u>	10.45	28.98%	6.83	11.12	31.12%	6.54	10.37	<u>29.44%</u>
	STAEFORMER [37]	1.7M	5.89	9.37	25.10%	6.52	10.52	29.00%	6.87	11.24	31.22%	6.56	10.39	29.84%
ConFormer			5.77	9.08	19.69%	6.40	10.23	23.16%	6.73	10.87	25.28%	6.37	10.22	23.13%
			1.4% ↑	2.9% ↑	19.7% ↑	1.4% ↑	2.9% ↑	20.8% ↑	1.2% ↑	2.2% ↑	19.5% ↑	1.7% ↑	1.2% ↑	21.5% ↑
DATA	METHOD	PARAM	45 MIN			90 MIN			180 MIN			AVERAGE		
			MAE	RMSE	MAPE	MAE	RMSE	MAPE	MAE	RMSE	MAPE	MAE	RMSE	MAPE
SAN DIEGO ($N = 716$) (ACCIDENT ✓)	LSTM [24]	98K	19.03	30.53	11.81%	25.84	40.87	16.44%	37.63	59.07	25.45%	26.44	41.73	17.20%
	AGCRN [4]	761K	15.71	27.85	11.48%	18.06	31.51	13.06%	21.86	39.44	16.52%	18.09	32.01	13.28%
	STGCN [66]	508K	17.45	29.99	12.42%	19.55	33.69	13.68%	23.21	41.23	16.32%	19.67	34.14	13.86%
	GWNET [62]	311K	15.35	25.17	10.67%	18.23	30.13	12.21%	22.44	38.02	15.69%	18.14	30.11	12.27%
	STGODE [16]	729K	16.75	28.04	11.00%	19.71	33.56	13.16%	23.67	42.12	16.58%	19.55	33.57	13.22%
	DSTAGNN [32]	3.9M	18.13	28.96	11.38%	21.71	34.44	13.93%	27.51	43.95	19.34%	21.82	34.68	14.40%
	STID [48]	258K	<u>15.14</u>	<u>25.07</u>	<u>9.84%</u>	<u>17.63</u>	<u>29.16</u>	<u>11.46%</u>	<u>21.02</u>	<u>36.72</u>	<u>15.02%</u>	<u>17.57</u>	<u>28.92</u>	<u>11.45%</u>
	DGCRN [34]	243K	15.34	25.35	10.01%	18.05	30.06	11.90%	22.06	37.51	15.27%	18.02	30.09	12.07%
	STAEFORMER [37]	1.7M	15.52	25.78	10.21%	18.23	30.66	12.20%	22.39	37.88	15.60%	18.21	30.44	12.27%
	D ² STGNN [49]	406K	15.58	25.74	10.55%	18.00	29.98	12.34%	21.96	37.10	15.06%	17.96	29.97	12.11%
ConFormer			14.52	24.33	9.24%	16.82	28.37	10.81%	20.18	34.53	13.52%	16.75	28.59	10.88%
			4.1% ↑	2.9% ↑	6.1% ↑	4.6% ↑	2.7% ↑	5.7% ↑	4.0% ↑	6.0% ↑	10.0% ↑	4.7% ↑	1.1% ↑	5.0% ↑
BAY AREA ($N = 2,352$) (ACCIDENT ✓)	LSTM [24]	98K	20.38	33.34	15.47%	27.56	43.57	23.52%	39.03	60.59	37.48%	27.96	44.21	24.48%
	AGCRN [4]	777K	18.31	30.24	14.27%	21.27	34.72	16.89%	25.85	40.18	20.80%	21.01	34.25	16.90%
	STGCN [66]	1.3M	21.05	34.51	16.42%	23.63	38.92	18.35%	26.87	44.45	21.92%	23.42	38.57	18.46%
	GWNET [62]	344K	17.85	29.12	13.92%	21.11	33.69	17.79%	25.58	40.19	23.48%	20.91	33.41	17.66%
	STGODE [16]	788K	18.84	30.51	15.43%	22.04	35.61	18.42%	26.22	42.90	22.83%	21.79	35.37	18.26%
	DSTAGNN [32]	26.9M	19.73	31.39	15.42%	24.21	37.70	20.99%	30.12	46.40	28.16%	23.82	37.29	20.16%
	DGCRN [34]	374K	18.02	29.49	14.13%	21.08	34.03	16.94%	25.25	40.63	21.15%	20.91	33.83	16.88%
	STID [48]	711K	<u>17.30</u>	<u>29.02</u>	13.56%	<u>20.47</u>	<u>33.34</u>	16.60%	<u>24.35</u>	<u>39.87</u>	20.60%	<u>20.19</u>	33.47	16.36%
	D ² STGNN [49]	446K	17.54	28.94	<u>12.12%</u>	20.92	33.92	<u>15.29%</u>	25.48	40.99	<u>19.83%</u>	20.71	33.65	<u>15.34%</u>
	STAEFORMER [37]	1.8M	17.58	29.04	12.59%	21.04	34.22	16.65%	25.86	40.52	20.42%	20.80	<u>33.37</u>	15.44%
ConFormer			16.93	28.48	12.09%	19.96	32.89	15.15%	24.03	39.06	19.68%	19.82	33.00	15.24%
			2.1% ↑	1.9% ↑	0.2% ↑	5.3% ↑	3.4% ↑	10.6% ↑	4.8% ↑	3.9% ↑	7.0% ↑	1.8% ↑	1.4% ↑	0.7% ↑

5 Experiment

5.1 Experimental Setup

Datasets. We collect large-scale traffic datasets along with accident and regulation information from both Tokyo and California. Details of the datasets are summarized in Table 1. The traffic accidents for both regions are visualized in Figure 1b. *We will release these datasets once the article is accepted.*

- First, we develop a comprehensive dataset encompassing 1,843 Tokyo expressway links over three months (October–December

2021). This dataset advances beyond existing collections [28] by incorporating authoritative incident data from the Japan Road Traffic Information Center (JARTIC) [26], maintained by Japan’s Ministry of Land, Infrastructure, Transport and Tourism. Our integration yields unprecedented 10-minute synchronized observations of traffic speeds, accidents, and regulatory interventions. The dataset captures fine-grained regulatory categories (single-lane restrictions, double-lane restrictions, road closures)

Table 3: Performance on the standard benchmarks, i.e., without using any accident information.

DATASET	METRIC	HI	STGCN [66]	DCRNN [35]	GWNNet [62]	AGCRN [4]	GTS [47]	STID [48]	PDFORMER [27]	STAEFORMER [37]	CONFORMER	IMPROVE	
PEMS03	AVERAGE	MAE	32.62	15.83	15.54	14.59	15.24	15.41	15.33	14.94	15.35	14.51	5.5% ↑
		RMSE	49.89	27.51	27.18	25.24	26.65	26.15	27.40	25.39	27.55	24.81	2.3% ↑
		MAPE	30.60%	16.13%	15.62%	15.52%	15.89%	15.39%	16.40%	15.82%	15.18%	14.38%	5.3% ↑
PEMS04	AVERAGE	MAE	42.35	19.57	19.63	18.53	19.38	20.96	18.38	18.36	18.22	17.89	1.8% ↑
		RMSE	61.66	31.38	31.26	29.92	31.25	32.95	29.95	30.03	30.18	29.79	1.3% ↑
		MAPE	29.92%	13.44%	13.59%	12.89%	13.40%	14.66%	12.04%	12.00%	11.98%	11.83%	1.3% ↑
PEMS07	AVERAGE	MAE	49.03	21.74	21.16	20.47	20.57	22.15	19.61	19.97	19.14	19.04	0.5% ↑
		RMSE	71.18	35.27	34.14	33.47	34.40	35.10	32.79	32.95	32.60	32.50	0.3% ↑
		MAPE	22.75%	9.24%	9.02%	8.61%	8.74%	9.38%	8.30%	8.55%	8.01%	7.89%	1.5% ↑
PEMS08	AVERAGE	MAE	36.66	16.08	15.22	14.40	15.32	16.49	14.21	13.58	13.46	13.32	1.0% ↑
		RMSE	50.45	25.39	24.17	23.39	24.41	26.08	23.28	23.41	23.25	22.96	1.2% ↑
		MAPE	21.63%	10.60%	10.21%	9.21%	10.03%	10.54%	9.27%	9.05%	8.88%	8.76%	1.4% ↑

and comprehensive accident classifications by severity (property damage, injury, fatality) and causative factors (overturns, collisions, fires, cargo collapse, debris, construction disruptions).

- Next, we systematically enhance California highway traffic data in San Diego (716 stations) and Bay Area (2,352 stations) published by LargeST [38], by incorporating the comprehensive U.S. Accidents dataset [43], containing 1.5 million georeferenced incident records across 49 states. These records, continuously collected since February 2016 from authoritative sources including MapQuest Traffic [2] and Microsoft Bing Map Traffic [1], provide detailed severity assessments from transportation departments, law enforcement, and traffic monitoring infrastructure.

Settings. Experiments were conducted on a GPU server with eight GeForce GTX 3090 GPUs using PyTorch 2.0.3. Data was standardized via z-score normalization [8]. Training employed early stopping, terminating if validation error stabilized within 15–20 epochs or showed no improvement after 200 epochs, with the best model retained based on validation performance [40]. Data was split chronologically into training, validation, and test sets in a 6:2:2 ratio. Model performance was evaluated using Mask-Based RMSE, MAE, and MAPE, excluding zero values as noise.

5.2 Performance Evaluation

Baselines. We included the following representative baselines in our study: Historical Inertia (HI) [36], a naive method that uses the average of historical values as the prediction result; LSTM [24], solely focusing on temporal aspects and ignoring spatial correlations; GNN-based models including DCRNN [35], AGCRN [4], STGCN [66], GWNNet [62], DSTAGNN [32], DGCRN [34], and D²STGNN [49]; Attention-based models including ASTGCN [21] and STTN [64]; Transformer variants such as PDFORMER [27] and STAEFORMER [37]; STGODE [16], a controlled differential equation-based method to model continuous traffic signal changes.

Performance on Our Datasets. Table 2 reports MAE, RMSE, and MAPE results for the Tokyo, Bay Area, and San Diego datasets across multiple prediction horizons, along with average performance. For the Tokyo dataset, following [28], the input and output lengths are set to $T = 6$ and $T' = 6$. For the Bay Area and San Diego datasets, following [38], the input and output lengths are $T = 12$ and $T' = 12$. GWNNet combines GNN and Gated TCN, while

DCRNN incorporates diffusion convolution into GRU. DGCRN extends DCRNN by modeling dynamic spatial topologies, achieving superior results among baselines. STAEFORMER excels in long-term predictions due to its ability to capture extended dependencies via attention mechanisms but faces scalability challenges on larger datasets like Bay Area. ConFORMER achieves SOTA performance across all datasets and prediction horizons, outperforming GCN-based methods (e.g., D²STGNN, GWNNet) and Transformer-based approaches (e.g., PDFORMER, STAEFORMER). The integration of global traffic context and conditional layer normalization contributes to its superior results. Crucially, ConFORMER is the first Transformer-based model capable of operating on very large graphs, demonstrating significant improvements and establishing Transformer’s scalability and effectiveness for large-scale traffic prediction.

Performance on Benchmarks. To further verify the performance of our method, we also conducted experiments on the widely-used benchmarks [21, 29] with input and output lengths are set to $T = 12$ and $T' = 12$. It is important to note that these benchmark datasets (PEMS03/04/07/08) do not contain traffic accident or regulation information, thus our ConFORMER model operates without these additional contextual inputs in these experiments. Table 3 presents the experimental results. ConFORMER consistently achieved the best performance across all ranges and datasets, demonstrating the effectiveness of our model. *The superior performance of ConFORMER on these traditional benchmarks demonstrates that our model can effectively utilize traffic flow signals as proxy variables for underlying traffic conditions through graph propagation, where the GLN mechanism and conditional attention architecture adaptively capture implicit disruptions and anomalies embedded within the spatiotemporal traffic patterns, even without explicit incident annotations.* The GLN mechanism enables dynamic adaptation to subtle variations in traffic patterns that may indicate implicit disruptions, while the conditional attention architecture learns to distinguish between regular flow fluctuations and anomalous conditions embedded within the spatiotemporal patterns. Through graph propagation, local traffic anomalies propagate across the network as measurable changes in flow characteristics, allowing ConFORMER to capture these implicit incident signatures even without explicit annotations.

Table 4: Comprehensive Ablation Studies

Variation	Component			Tokyo			San Diego		Bay Area	
	Spatial	Temporal	LN	Normal	Accident	Regulation	Normal	Accident	Normal	Accident
ConFormer	Attention	Attention	GLN	6.37	8.98	9.18	16.75	22.36	19.82	26.95
Module	Attention	Attention	w/ LN	6.45	9.58	9.30	16.86	23.49	19.96	28.45
	w/ MLP	w/ MLP	GLN	6.75	10.06	9.42	17.39	24.19	20.57	29.30
	Attention	w/o	GLN	6.55	9.34	9.53	17.10	22.81	20.23	27.49
	w/o	Attention	GLN	6.75	9.42	9.65	17.16	23.01	20.27	27.55
	Attention	Attention	w/o α	6.48	9.15	9.53	16.95	22.45	19.99	27.08
	Attention	Attention	w/o β	6.44	9.33	9.53	16.81	23.68	19.92	28.15
	Attention	Attention	w/o γ	6.46	9.42	9.53	16.80	23.49	19.96	28.33
Data	w/o Accident		GLN	6.39	10.97	10.12	16.81	23.27	19.87	28.17
	w/o Regulation		GLN	6.41	9.48	10.64	-	-	-	-

Table 5: Performance of GLN on GWNNet

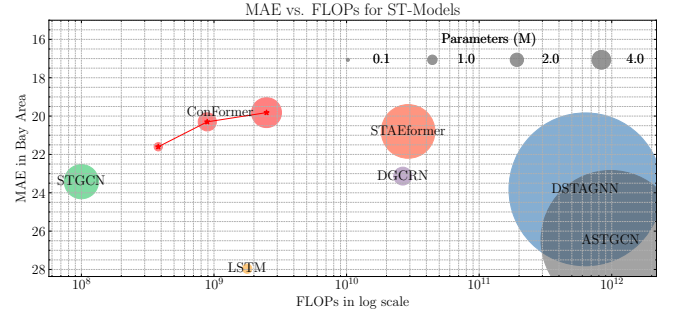
Model	Tokyo		San Diego		Bay Area	
	MAE	RMSE	MAE	RMSE	MAE	RMSE
GWNNet	20.91	33.41	18.14	30.11	6.56	10.40
GLN+GWNNet	20.25	32.74	17.64	29.45	6.43	10.21

5.3 Ablation Study

Through comprehensive ablation studies, we systematically evaluated the contribution of each component in ConFormer. The baseline ConFormer, integrating spatial attention, temporal attention, and GLN, consistently achieves optimal performance across all datasets and scenarios. Detailed ablation experiments were conducted from four aspects: (1) Replacing GLN with standard layer normalization leads to notable performance degradation (MAE increases from 8.98 to 9.58 in accident scenarios), while substituting attention mechanisms with MLPs results in more significant deterioration (MAE rises to 10.06), validating the necessity of our attention-based architecture. (2) Further experiments removing individual components (w/o) show that both spatial and temporal attention are crucial. Removing either causes performance drops across all datasets. For example, on the Tokyo dataset, removing temporal attention increases MAE from 6.37 to 6.55, and removing spatial attention raises it to 6.75. (3) Each modulation factor (α , β , γ) in GLN plays a distinct role in enhancing model performance:

- α primarily affects model optimization, influencing performance in both normal and accident scenarios (removing it increases MAE from 16.75 to 16.95 on San Diego dataset).
- β increases model sensitivity to sudden traffic disruptions (its removal leads to MAE increase from 22.36 to 23.68 in accident scenarios).
- γ captures node-specific conditions to distinguish between normal and accident scenarios (removing it increases MAE from 26.95 to 28.33 in Bay Area accident cases).

(4) we evaluated the importance of incorporating accident and regulation data. Removing accident information substantially impairs prediction accuracy in corresponding scenarios (MAE increases from 8.98 to 10.97 in Tokyo accident scenarios). Similarly, removing regulation data leads to worse performance in regulation scenarios

**Figure 3: Comparison of model efficiency and effectiveness across spatiotemporal models on the Bay Area dataset.**

(MAE increases from 9.18 to 10.64). This empirically validates the effectiveness of incorporating traffic incident information.

Besides, to validate the extensibility of our method, we implemented a condition-informed variant of GWNNet, denoted as GLN+GWNNet, and evaluated it across three datasets. As presented in Table 5, notably, GLN+GWNNet achieved a 2.63% reduction in MAE compared to the original GWNNet across all datasets.

5.4 Efficiency Evaluation

Figure 3 compares the efficiency and effectiveness of various spatiotemporal models on the Bay Area dataset. The x-axis shows computational complexity (FLOPs) on a logarithmic scale, the y-axis denotes predictive accuracy (MAE, with lower values indicating better performance), and circle size denotes model parameters (in millions, M). ConFormer demonstrates a notable balance between accuracy and computational cost, with MAE improving clearly as model complexity increases. STGCN achieves relatively low MAE with minimal computational overhead, while LSTM has the lowest complexity but poor accuracy. In contrast, ConFormer stands out by efficiently enhancing prediction performance with moderate increases in complexity. DSTAGNN and ASTGCN, however, achieve competitive accuracy at the cost of significantly higher computational demands and parameter counts.

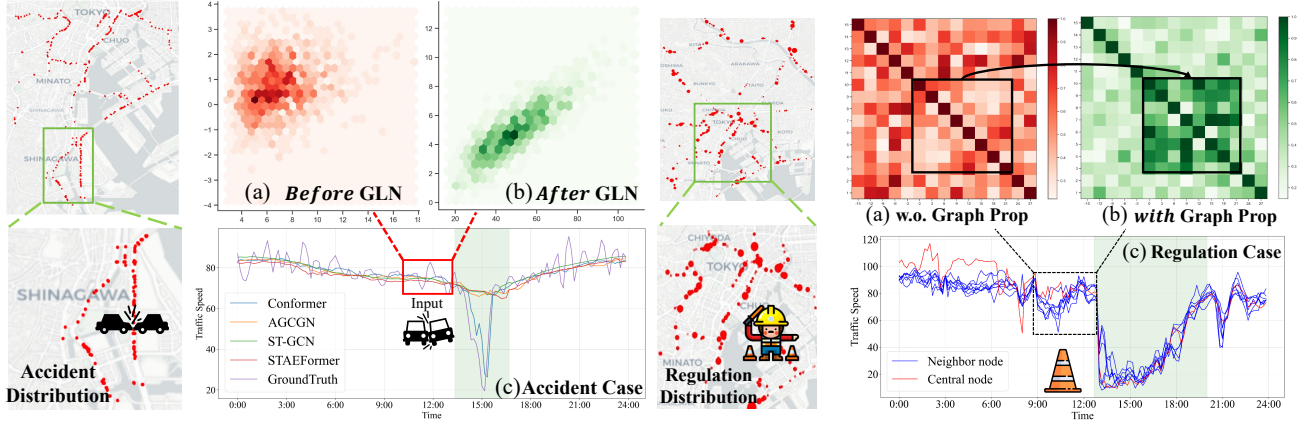


Figure 4: Case studies of traffic prediction in a subarea of Tokyo. Left: Analysis of an accident scenario, where ConFormer effectively captures the evolution of node distributions in latent space before and after the accident. Right: Analysis of a traffic regulation scenario, where graph propagation demonstrates learned differential attention scores in response to the implemented traffic regulations.

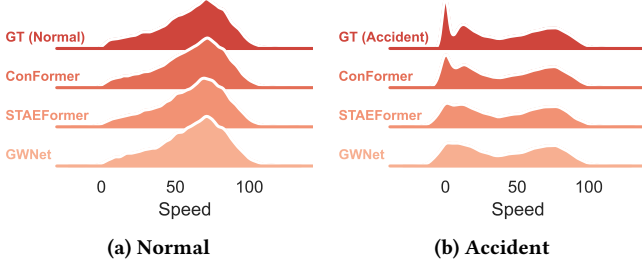


Figure 5: Distribution of predictions and ground-truths under normal and accident scenarios on Tokyo dataset.

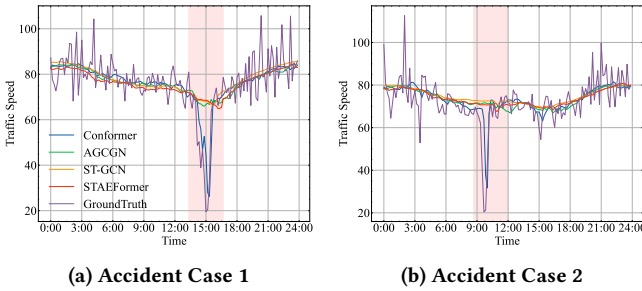


Figure 6: Prediction results of two accident cases on Tokyo.

5.5 Case Study

Using the Tokyo dataset, we conducted several specific case analyses: (1) For the **traffic accident scenario** (Figure 4-left), our analysis showed that ConFormer effectively captures the evolving patterns of node distributions in the latent space. Using t-SNE dimensionality reduction, we visualized the feature spaces before and after the accident—before the accident, traffic time series showed normal, uncongested patterns, with tightly linked features among neighboring nodes. This hinders traditional models’ ability to predict accidents; however, ConFormer uses the GLN mechanism with

parameters γ_c and β to induce significant feature shifts, enabling more accurate differentiation of abnormal traffic conditions. (2) For the **traffic regulation scenario** (Figure 4-right), we also tested the model’s ability to transmit information and adapt to traffic changes. The central node implemented traffic regulations from 13:00 to 20:00: before the regulations, there was a clear difference in attention distribution between the central node and its neighbors; after the regulations began, the speeds of these nodes became highly consistent. This highlights the critical role of graph propagation in helping the model adapt to and transmit traffic information—through conditional mapping message passing, the attention maps of the central node and its neighbors show significantly enhanced correlation, demonstrating ConFormer’s ability to dynamically respond to changes in the traffic environment.

As shown in Figure 5, we compare ConFormer, STAEFormer, and GWNNet predictions against ground-truth distributions for normal and accident scenarios on the Tokyo dataset. ConFormer demonstrates superior performance in accident scenarios while maintaining comparable accuracy in normal conditions, particularly excelling at handling sudden traffic disruptions.

Figure 6 presents two case studies from the Tokyo dataset—two traffic accidents and two traffic regulations—comparing ConFormer against AGCGN, ST-GCN, STAEFormer, and ground truth. In both accident cases (Figure 6a and Figure 6b), ConFormer accurately captured the traffic velocity drops at 12:00 and 09:00 respectively, significantly outperforming competing models in predicting these sudden deceleration patterns.

5.6 Hyperparameter Study

We evaluated the sensitivity of the ConFormer architecture to key hyperparameters using the Tokyo dataset (Figure 7). The analysis covered input embedding dimension (D_{data}), spatiotemporal attention dimension (D_{stae}), daily and weekly pattern dimensions (D_d , D_w), accident and regulation dimensions (D_{acc} , D_{reg}), and graph propagation order (k). Results show optimal performance with embedding dimensions between 8 and 16, with D_{data} and D_{stae} being

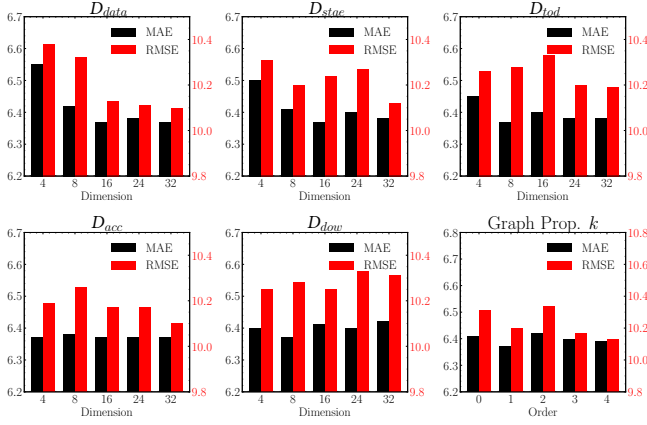


Figure 7: Hyperparameter study on Tokyo dataset.

most critical, while D_{acc} and D_{reg} had minimal impact. Shallow graph propagation (order 1–2) effectively captured spatial dependencies, with limited benefit from higher orders. These findings highlight ConFormer’s robustness and efficiency, ensuring adaptability to real-world scenarios with constrained resources.

6 Conclusion

This paper introduces ConFormer, a novel conditional Transformer architecture for traffic prediction. By incorporating graph-based propagation adaptive normalization layers, ConFormer dynamically adjusts spatial and temporal correlations based on historical conditions. We validate our approach using two new datasets from Tokyo and California, demonstrating consistent superiority over mainstream spatio-temporal baselines. ConFormer exhibits exceptional performance on both traditional PEMS benchmarks and our newly collected large-scale datasets with traffic incident information.

References

- [1] 2019. Bing Map Traffic API. <https://www.bingmapsportal.com/>. Accessed: 2019-05-05.
- [2] 2019. MapQuest Traffic API. <https://www.mapquest.com/>. Accessed: 2019-05-05.
- [3] Jimmy Lei Ba, Jamie Ryan Kiros, and Geoffrey E Hinton. 2016. Layer normalization. *arXiv preprint arXiv:1607.06450* (2016).
- [4] Lei Bai, Lina Yao, Can Li, Xianzhi Wang, and Can Wang. 2020. Adaptive graph convolutional recurrent network for traffic forecasting. *Advances in neural information processing systems* 33, 17804–17815.
- [5] Shai Ben-David, John Blitzer, Koby Crammer, Alex Kulesza, Fernando Pereira, and Jennifer Wortman Vaughan. 2010. A theory of learning from different domains. *ML* (2010).
- [6] Yoshua Bengio, Jérôme Louradour, Ronan Collobert, and Jason Weston. 2009. Curriculum learning. In *Proceedings of the 26th annual international conference on machine learning*. 41–48.
- [7] Defu Cao, Yujing Wang, Juanyong Duan, Ce Zhang, Xia Zhu, Congrui Huang, Yunhai Tong, Bixiong Xu, Jing Bai, Jie Tong, et al. 2020. Spectral temporal graph neural network for multivariate time-series forecasting. *Advances in neural information processing systems* 33, 17766–17778.
- [8] Chris Cheshire, Marquis P Vawter, William J Freed, and Kevin G Becker. 2003. Analysis of microarray data using Z score transformation. *The Journal of molecular diagnostics* 5, 2 (2003), 73–81.
- [9] Peng Chen, Yingying Zhang, Yunyao Cheng, Yang Shu, Yihang Wang, Qingsong Wen, Bin Yang, and Chenjuan Guo. 2024. Multi-scale Transformers with Adaptive Pathways for Time Series Forecasting. In *International Conference on Learning Representations*.
- [10] Junyoung Chung, Caglar Gulcehre, KyungHyun Cho, and Yoshua Bengio. 2014. Empirical evaluation of gated recurrent neural networks on sequence modeling. *arXiv preprint arXiv:1412.3555* (2014).
- [11] Younshik Chung. 2011. Quantification of nonrecurrent congestion delay caused by freeway accidents and analysis of causal factors. *Transportation Research Record* 2229, 1 (2011), 8–18. Provides quantitative analysis of nonrecurrent congestion delays from freeway accidents.
- [12] Gary A Davis and Nancy L Nihan. 1991. Nonparametric regression and short-term freeway traffic forecasting. *Journal of Transportation Engineering* 117, 2 (1991), 178–188.
- [13] Michaël Defferrard, Xavier Bresson, and Pierre Vandergheynst. 2016. Convolutional neural networks on graphs with fast localized spectral filtering. In *Proceedings of Advances in Neural Information Processing Systems*. 3837–3845.
- [14] Jinliang Deng, Xiuxi Chen, Renhe Jiang, Xuan Song, and Ivor W Tsang. 2021. Stnorm: Spatial and temporal normalization for multi-variate time series forecasting. In *Proceedings of the 27th ACM SIGKDD Conference on Knowledge Discovery & Data Mining*. 269–278.
- [15] Zheng Dong, Renhe Jiang, Haotian Gao, Hangchen Liu, Jinliang Deng, Qingsong Wen, and Xuan Song. 2024. Heterogeneity-informed Meta-parameter Learning for Spatiotemporal Time Series Forecasting. In *Proceedings of the 30th ACM SIGKDD Conference on Knowledge Discovery and Data Mining*. 631–641.
- [16] Zheng Fang, Qingqing Long, Guojie Song, and Kunqing Xie. 2021. Spatial-temporal graph ode networks for traffic flow forecasting. In *Proceedings of the 27th ACM SIGKDD Conference on Knowledge Discovery & Data Mining*. 364–373.
- [17] Federal Highway Administration. 2005. *Traffic Congestion and Reliability: Trends and Advanced Strategies for Congestion Mitigation*. Technical Report. U.S. Department of Transportation, Federal Highway Administration, Washington, DC. https://ops.fhwa.dot.gov/congestion_report/executive_summary.htm Reports that when traffic incidents and weather events are present, travel times can increase by up to 43% compared to average conditions, based on data from State Route 520 in Seattle.
- [18] Federal Highway Administration Office of Operations. 2004. *Traffic Congestion and Reliability: Linking Solutions to Problems*. Technical Report. U.S. Department of Transportation, Federal Highway Administration, Washington, DC. https://ops.fhwa.dot.gov/congestion_report_04/chapter3.htm Documents travel time increases of 37% during incident discovery scenarios compared to normal conditions.
- [19] Haotian Gao, Renhe Jiang, Zheng Dong, Jinliang Deng, Yuxuan Ma, and Xuan Song. 2024. Spatial-Temporal-Decoupled Masked Pre-training for Spatiotemporal Forecasting. In *Proceedings of the 33rd International Joint Conference on Artificial Intelligence*.
- [20] P Goyal. 2017. Accurate, large minibatch SG D: training imagenet in 1 hour. *arXiv preprint arXiv:1706.02677* (2017).
- [21] Shengnan Guo, Youfang Lin, Ning Feng, Chao Song, and Huaiyu Wan. 2019. Attention based spatial-temporal graph convolutional networks for traffic flow forecasting. In *Proceedings of the AAAI conference on artificial intelligence*, Vol. 33. 922–929.
- [22] Filmon G Habtemichael, Mecit Cetin, and Khairul A Anuar. 2015. Incident-induced delays on freeways. *Transportation Research Record* 2484, 1 (2015), 60–68. Demonstrates that freeway incidents cause nonrecurrent congestion contributing significantly to overall travel delays.
- [23] Jindong Han, Weijia Zhang, Hao Liu, Tao Tao, Naiqiang Tan, and Hui Xiong. 2024. Bigst: Linear complexity spatio-temporal graph neural network for traffic forecasting on large-scale road networks. *Proceedings of the VLDB Endowment* 17, 5 (2024), 1081–1090.
- [24] Sepp Hochreiter and Jürgen Schmidhuber. 1997. Long short-term memory. *Neural computation* 9, 8 (1997), 1735–1780.
- [25] Lee Hyunwook and Ko Sungahn. 2024. TESTAM: A Time-Enhanced Spatio-Temporal Attention Model with Mixture of Experts. In *The Twelfth International Conference on Learning Representations*.
- [26] Japan Road Traffic Information Center. 2025. Japan Road Traffic Information Center: JARTIC. <https://www.jartic.or.jp/> Official website of Japan Road Traffic Information Center.
- [27] Jiawei Jiang, Chengkai Han, Wayne Xin Zhao, and Jingyuan Wang. 2023. PDFormer: Propagation Delay-aware Dynamic Long-range Transformer for Traffic Flow Prediction. In *AAAI AAAI Press*.
- [28] Renhe Jiang, Zhaonan Wang, Jiawei Yong, Puneet Jeph, Quanjuan Chen, Yashumasa Kobayashi, Xuan Song, Shintaro Fukushima, and Toyotaro Suzumura. 2023. Spatio-temporal meta-graph learning for traffic forecasting. In *Proceedings of the AAAI Conference on Artificial Intelligence*, Vol. 37. 8078–8086.
- [29] Renhe Jiang, Du Yin, Zhaonan Wang, Yizhuo Wang, Jiewen Deng, Hangchen Liu, Zekun Cai, Jinliang Deng, Xuan Song, and Ryosuke Shibasaki. 2021. DL-traffic: Survey and benchmark of deep learning models for urban traffic prediction. In *Proceedings of the 30th ACM international conference on information & knowledge management*. 4515–4525.
- [30] Angelos Katharopoulos, Apoorv Vyas, Nikolaos Pappas, and François Fleuret. 2020. Transformers are rnns: Fast autoregressive transformers with linear attention. In *International conference on machine learning*. PMLR, 5156–5165.
- [31] Thomas N Kipf and Max Welling. 2017. Semi-supervised classification with graph convolutional networks. In *International Conference on Learning Representations*.
- [32] Shiyong Lan, Yitong Ma, Weikang Huang, Wenwu Wang, Hongyu Yang, and Pyang Li. 2022. Dstagnn: Dynamic spatial-temporal aware graph neural network

- for traffic flow forecasting. In *International conference on machine learning*. PMLR, 11906–11917.
- [33] Hyunwook Lee, Seungmin Jin, Hyeshin Chu, Hongkyu Lim, and Sungahn Ko. 2022. Learning to Remember Patterns: Pattern Matching Memory Networks for Traffic Forecasting. In *International Conference on Learning Representations*.
 - [34] Fuxian Li, Jie Feng, Huan Yan, Guangyin Jin, Fan Yang, Funing Sun, Depeng Jin, and Yong Li. 2023. Dynamic graph convolutional recurrent network for traffic prediction: Benchmark and solution. *ACM Transactions on Knowledge Discovery from Data* 17, 1 (2023), 1–21.
 - [35] Yaguang Li, Rose Yu, Cyrus Shahabi, and Yan Liu. 2018. Diffusion Convolutional Recurrent Neural Network: Data-Driven Traffic Forecasting. In *International Conference on Learning Representations*.
 - [36] Yuxuan Liang, Kun Ouyang, Yiwei Wang, Ye Liu, Junbo Zhang, Yu Zheng, and David S Rosenblum. 2021. Revisiting convolutional neural networks for citywide crowd flow analytics. In *Proceedings of European Conference on Machine Learning and Principles and Practice of Knowledge Discovery*. 578–594.
 - [37] Hangchen Liu, Zheng Dong, Renhe Jiang, Jiewen Deng, Jinliang Deng, Qun-jun Chen, and Xuan Song. 2023. Spatio-temporal adaptive embedding makes vanilla transformer sota for traffic forecasting. In *Proceedings of the 32nd ACM International Conference on Information and Knowledge Management*. 4125–4129.
 - [38] Xu Liu, Yutong Xia, Yuxuan Liang, Junfeng Hu, Yiwei Wang, Lei Bai, Chao Huang, Zhengguang Liu, Bryan Hooi, and Roger Zimmermann. 2023. LargeST: A Benchmark Dataset for Large-Scale Traffic Forecasting. *arXiv preprint arXiv:2306.08259* (2023).
 - [39] Yong Liu, Tengge Hu, Haoran Zhang, Haixu Wu, Shiyu Wang, Lintao Ma, and Mingsheng Long. 2023. iTransformer: Inverted Transformers Are Effective for Time Series Forecasting. *arXiv preprint arXiv:2310.06625* (2023).
 - [40] Xunlian Luo, Chunjiang Zhu, Detian Zhang, and Qing Li. 2023. Dynamic Graph Convolution Network with Spatio-Temporal Attention Fusion for Traffic Flow Prediction. *arXiv preprint arXiv:2302.12598* (2023).
 - [41] Zhongjian Lv, Jiajie Xu, Kai Zheng, Hongzhi Yin, Pengpeng Zhao, and Xiaofang Zhou. 2018. Lc-rnn: A deep learning model for traffic speed prediction.. In *IJCAI*, Vol. 2018. 27th.
 - [42] Xiaolei Ma, Zhimin Tao, Yinhai Wang, Haiyang Yu, and Yunpeng Wang. 2015. Long short-term memory neural network for traffic speed prediction using remote microwave sensor data. *Transportation Research Part C: Emerging Technologies* 54 (2015).
 - [43] Sobhan Moosavi, Mohammad Hossein Samavatian, Srinivasan Parthasarathy, and Rajiv Ramnath. 2019. A countrywide traffic accident dataset. *arXiv preprint arXiv:1906.05409* (2019).
 - [44] Bei Pan, Ugur Demiryurek, and Cyrus Shahabi. 2012. Utilizing real-world transportation data for accurate traffic prediction. In *2012 IEEE 12th international conference on data mining*. IEEE, 595–604.
 - [45] Taesung Park, Ming-Yu Liu, Ting-Chun Wang, and Jun-Yan Zhu. 2019. Semantic image synthesis with spatially-adaptive normalization. In *CVPR*.
 - [46] Robin Rombach, Andreas Blattmann, Dominik Lorenz, Patrick Esser, and Björn Ommer. 2022. High-resolution image synthesis with latent diffusion models. In *Proceedings of the IEEE/CVF conference on computer vision and pattern recognition*. 10684–10695.
 - [47] Chao Shang, Jie Chen, and Jinbo Bi. 2021. Discrete Graph Structure Learning for Forecasting Multiple Time Series. In *International Conference on Learning Representations*.
 - [48] Zezhi Shao, Zhao Zhang, Fei Wang, Wei Wei, and Yongjun Xu. 2022. Spatial-temporal identity: A simple yet effective baseline for multivariate time series forecasting. In *Proceedings of the 31st ACM International Conference on Information & Knowledge Management*. 4454–4458.
 - [49] Zezhi Shao, Zhao Zhang, Wei Wei, Fei Wang, Yongjun Xu, Xin Cao, and Christian S Jensen. 2022. Decoupled dynamic spatial-temporal graph neural network for traffic forecasting. *Proceedings of the VLDB Endowment* 15, 11 (2022), 2733–2746.
 - [50] James H Stock and Mark W Watson. 2001. Vector autoregressions. *Journal of Economic perspectives* 15, 4 (2001), 101–115.
 - [51] Lelitha Vanajakshi and Laurence R Rilett. 2004. A comparison of the performance of artificial neural networks and support vector machines for the prediction of traffic speed. In *IEEE Intelligent Vehicles Symposium, 2004*. IEEE, 194–199.
 - [52] Hongjun Wang, Jiyuan Chen, Zipei Fan, Zhiwen Zhang, Zekun Cai, and Xuan Song. 2022. St-expertnet: A deep expert framework for traffic prediction. *IEEE Transactions on Knowledge and Data Engineering* (2022).
 - [53] Hongjun Wang, Jiyuan Chen, Tong Pan, Zheng Dong, Lingyu Zhang, Renhe Jiang, and Xuan Song. 2024. STGformer: Efficient Spatiotemporal Graph Transformer for Traffic Forecasting. *arXiv preprint arXiv:2410.00385* (2024).
 - [54] Hongjun Wang, Jiyuan Chen, Tong Pan, Zipei Fan, Xuan Song, Renhe Jiang, Lingyu Zhang, Yi Xie, Zhongyi Wang, and Boyuan Zhang. 2023. Easy Begun Is Half Done: Spatial-Temporal Graph Modeling with ST-Curriculum Dropout. In *Proceedings of the AAAI Conference on Artificial Intelligence*, Vol. 37. 4668–4675.
 - [55] Sinong Wang, Belinda Z Li, Madian Khabsa, Han Fang, and Hao Ma. 2020. Linformer: Self-attention with linear complexity. *arXiv preprint arXiv:2006.04768* (2020).
 - [56] Xiaoyang Wang, Yao Ma, Yiqi Wang, Wei Jin, Xin Wang, Jiliang Tang, Caiyan Jia, and Jian Yu. 2020. Traffic flow prediction via spatial temporal graph neural network. In *Proceedings of the web conference 2020*. 1082–1092.
 - [57] Zhaonan Wang, Renhe Jiang, Zekun Cai, Zipei Fan, Xin Liu, Kyoung-Sook Kim, Xuan Song, and Ryosuke Shibasaki. 2021. Spatio-Temporal-Categorical Graph Neural Networks for Fine-Grained Multi-Incident Co-Prediction. In *Proceedings of the 30th ACM International Conference on Information & Knowledge Management*. 2060–2069.
 - [58] Qingsong Wen, Tian Zhou, Chaoli Zhang, Weiqi Chen, Ziqing Ma, Junchi Yan, and Liang Sun. 2023. Transformers in time series: A survey. In *International Joint Conference on Artificial Intelligence (IJCAI)*.
 - [59] Haixu Wu, Jiehui Xu, Jianmin Wang, and Mingsheng Long. 2021. Autoformer: De-composition transformers with auto-correlation for long-term series forecasting. *Advances in Neural Information Processing Systems* 34 (2021), 22419–22430.
 - [60] Qitian Wu, Wentao Zhao, Chenxiao Yang, Hengrui Zhang, Fan Nie, Haitian Jiang, Yatao Bian, and Junchi Yan. 2024. Simplifying and empowering transformers for large-graph representations. *Advances in Neural Information Processing Systems* 36 (2024).
 - [61] Zonghan Wu, Shirui Pan, Guodong Long, Jing Jiang, Xiaojun Chang, and Chengqi Zhang. 2020. Connecting the dots: Multivariate time series forecasting with graph neural networks. In *Proceedings of the 26th ACM SIGKDD international conference on knowledge discovery & data mining*. 753–763.
 - [62] Zonghan Wu, Shirui Pan, Guodong Long, Jing Jiang, and Chengqi Zhang. 2019. Graph wavenet for deep spatial-temporal graph modeling. In *Proceedings of the 28th International Joint Conference on Artificial Intelligence*. 1907–1913.
 - [63] Yutong Xia, Yuxuan Liang, Haomin Wen, Xu Liu, Kun Wang, Zhengyang Zhou, and Roger Zimmermann. 2023. Deciphering Spatio-Temporal Graph Forecasting: A Causal Lens and Treatment. (2023).
 - [64] Mingxing Xu, Wenrui Dai, Chunmiao Liu, Xing Gao, Weiyao Lin, Guo-Jun Qi, and Hongkai Xiong. 2020. Spatial-temporal transformer networks for traffic flow forecasting. *arXiv preprint arXiv:2001.02908* (2020).
 - [65] Ling Yang, Zhilong Zhang, Yang Song, Shenda Hong, Runsheng Xu, Yue Zhao, Wentao Zhang, Bin Cui, and Ming-Hsuan Yang. 2023. Diffusion models: A comprehensive survey of methods and applications. *Comput. Surveys* 56, 4 (2023), 1–39.
 - [66] Bing Yu, Haoteng Yin, and Zhanxing Zhu. 2018. Spatio-temporal graph convolutional networks: a deep learning framework for traffic forecasting. In *Proceedings of the 27th International Joint Conference on Artificial Intelligence*. 3634–3640.
 - [67] Yingxue Zhang, Yanhua Li, Xun Zhou, Xiangnan Kong, and Jun Luo. 2020. Curbgan: Conditional urban traffic estimation through spatio-temporal generative adversarial networks. In *Proceedings of the 26th ACM SIGKDD International Conference on Knowledge Discovery & Data Mining*. 842–852.
 - [68] Yu Zhang, Guojie Shen, Weixing Zhang, Ke Ning, Renhe Jiang, and Xiangjie Kong. 2025. Uncertainty-aware traffic accident risk prediction via multi-view hypergraph contrastive learning. *Information Fusion* 103 (2025), 103331.
 - [69] Chuanpan Zheng, Xiaoliang Fan, Cheng Wang, and Jianzhong Qi. 2020. Gman: A graph multi-attention network for traffic prediction. In *Proceedings of the AAAI conference on artificial intelligence*, Vol. 34. 1234–1241.
 - [70] Haoyi Zhou, Shanghang Zhang, Jieqi Peng, Shuai Zhang, Jianxin Li, Hui Xiong, and Wancai Zhang. 2021. Informer: Beyond efficient transformer for long sequence time-series forecasting. In *Proceedings of the AAAI conference on artificial intelligence*, Vol. 35. 11106–11115.
 - [71] Tian Zhou, Ziqing Ma, Qingsong Wen, Xue Wang, Liang Sun, and Rong Jin. 2022. Fedformer: Frequency enhanced decomposed transformer for long-term series forecasting. In *International Conference on Machine Learning*. PMLR, 27268–27286.
 - [72] Zhengyang Zhou, Yang Wang, Xike Xie, Lianliang Chen, and Chaochao Zhu. 2022. Foresee Urban Sparse Traffic Accidents: A Spatiotemporal Multi-Granularity Perspective. *IEEE Transactions on Knowledge and Data Engineering* 34, 8 (2022), 3757–3770.

A Appendix

A.1 Dataset Details

We use this traffic accident dataset [43] covering 49 states in the United States to match California’s traffic network in Caltrans Performance Measurement System (PEMS) with traffic accident data. This dataset has been collecting data from multiple data providers since February 2016. These data providers include multiple APIs that provide real-time traffic incident data streams. The traffic incidents broadcast by these APIs are captured by various entities, such

as US and state transportation departments, law enforcement agencies, traffic cameras, and traffic sensors within the road network. Currently, the dataset contains about 1.5 million accident records.

Compared with PEMS dataset, Tokyo provides traffic regulations and accidents, which includes fields for various types of lane restrictions, such as single lane restriction, double lane restriction, no restriction, under restriction, general lane restriction, and road closure. The dataset also records the causes of accidents, including overturned vehicle accidents, broken-down vehicles, accidents, vehicle fires, collision accidents, contact accidents, and rear-end collisions. An regulations dataset, includes additional causes such as cargo collapse, unknown causes, construction, scattered objects, earthquakes, falling objects, and road obstructions, along with a new regulation category for traffic jams. This dataset is instrumental for analyzing traffic accidents, understanding road conditions, and enhancing traffic management and safety measures.

A.2 Training Details

Our experiments ran on a GPU server with eight GeForce GTX 3090 graphics cards, employing the PyTorch 2.0.3 framework. The raw data was standardized using z-score normalization [8]. Training was halted prematurely if validation error stabilized within 15-20 epochs or did not improve after 200 epochs, preserving the best model based on validation data [40]. We adhered to the original paper’s model parameters and settings, while also conducting multiple parameter tuning iterations to enhance experimental outcomes. Data were partitioned chronologically into training, validation, and test sets at a 6:2:2 ratio across all sub-datasets. Model performance was assessed using Mask-Based Root Mean Square Error (RMSE), Mean Absolute Error (MAE), and Mean Absolute Percentage Error (MAPE) as metrics, disregarding zero values which indicated noisy data [28]. Recent research [38] indicates that existing Graph Convolutional Networks (GCNs) and Transformer-based methods are largely inadequate for real-world road networks, particularly for large graphs exceeding 2000 nodes, due to the prohibitive computational costs associated with capturing both global and local traffic patterns. As illustrated in Figure 2, the majority of methods encounter out-of-memory errors when applied to the Bay Area dataset, which spans a one-year period. To address this challenge, we have implemented efficient linear attention mechanisms [30, 55, 60] on the Bay Area dataset. These mechanisms are designed to mitigate the substantial resource demands of traditional dot-product attention, which exhibits quadratic memory and computational complexity. The high computational and memory costs render dot-product attention impractical for real-world traffic networks. Our findings demonstrate that the utilization of linear attention does not compromise model performance.

A.3 Baseline Details

We included the following representative baselines in our study: Historical Last (HL) [36]: A naive method that uses the average of historical values as the prediction result. LSTM [24]: Focuses solely on temporal aspects, ignoring spatial correlations. For methods combining GNNs [13, 31], we considered: RNN-based approaches such as DCRNN [35] and AGCRN [4]. TCN-based methods like STGCN [66] and GWNET [62]. Attention-based models including ASTGCN

[21] and STTN [64]. Transformer variants such as PDFormer [27] and STAEFormer [37]. Additionally, we integrated more sophisticated techniques: Controlled differential-based method: STGODE [16] uses neural ordinary differential equations to model continuous traffic signal changes. Dynamic graph-based methods: These include DSTAGNN [32], DGCRN [34], and D²STGNN [49], which specifically address dynamic correlations among sensors in traffic networks.

A.4 Proof of Reformulated Self-Attention

With GLN, the vanilla self-attention can be reformulated as follows:

$$\text{Softmax}\left(\frac{\mathbf{Q}\mathbf{K}^\top}{\sqrt{D_k}}\right) \rightarrow \text{Softmax}\left(\frac{\gamma^2 \mathbf{Q}'\mathbf{K}'^\top + \gamma \mathbf{K}'\beta^\top + \gamma \mathbf{Q}'\beta^\top + \beta^2}{\sqrt{D_k}}\right) \quad (1)$$

where $\mathbf{Q}' = \gamma \cdot \frac{\mathbf{Q} - \mu_{\mathbf{Q}}}{\sigma}$ and $\mathbf{K}' = \gamma \cdot \frac{\mathbf{K} - \mu_{\mathbf{K}}}{\sigma} + \beta$.

PROOF. We proceed through several key steps to establish this theorem, leveraging the properties of Generalized Layer Normalization (GLN) and the linearity of the embedding layer.

- **Normalization of Input:** For an input x , the normalized version using GLN with conditional affine transformation parameters γ and β is given by:

$$x'_i = \gamma \cdot \frac{x_i - \mu_i}{\sigma_i} + \beta,$$

where μ_i and σ_i represent the mean and standard deviation of x_i , respectively.

- **Linear Embedding Transformation:** Given the linearity of the embedding layer, denoted by function f , we can express the normalized input as:

$$q'_i = \gamma \cdot \frac{f(x_i) - f(\mu_i)}{\sigma_i} + f(\beta),$$

where we define $\mu_{q_i} = f(\mu_i)$ and $\sigma_{q_i} = \sigma_i$. Thus, q'_i can be rewritten as:

$$q'_i = \gamma \cdot \frac{q_i - \mu_{q_i}}{\sigma_i} + \beta, \quad \text{where } \beta = f(\beta).$$

- **Formulation of \mathbf{Q}' and \mathbf{K}' :**

$$\mathbf{Q}' = \gamma \cdot \frac{\mathbf{Q} - \mu_{\mathbf{Q}}}{\sigma} + \beta, \quad \mathbf{K}' = \gamma \cdot \frac{\mathbf{K} - \mu_{\mathbf{K}}}{\sigma} + \beta.$$

- **Computation of $\mathbf{Q}'\mathbf{K}'^\top$:**

$$\mathbf{Q}'\mathbf{K}'^\top = \left(\gamma \cdot \frac{\mathbf{Q} - \mu_{\mathbf{Q}}}{\sigma} + \beta\right) \left(\gamma \cdot \frac{\mathbf{K} - \mu_{\mathbf{K}}}{\sigma} + \beta\right)^\top$$

- **Expansion of $\mathbf{Q}'\mathbf{K}'^\top$:**

$$\mathbf{Q}'\mathbf{K}'^\top = \gamma^2 \left(\frac{\mathbf{Q} - \mu_{\mathbf{Q}}}{\sigma}\right) \left(\frac{\mathbf{K} - \mu_{\mathbf{K}}}{\sigma}\right)^\top + \gamma \beta \left(\frac{\mathbf{K} - \mu_{\mathbf{K}}}{\sigma}\right)^\top + \gamma \left(\frac{\mathbf{Q} - \mu_{\mathbf{Q}}}{\sigma}\right) \beta^\top + \beta^2.$$

- **Formulation of the Softmax Attention:**

Substituting this expanded form into the Self-Attention formula, we arrive at:

$$\text{Softmax}\left(\frac{\mathbf{Q}\mathbf{K}^\top}{\sqrt{D_k}}\right) = \text{Softmax}\left(\frac{\gamma^2 \mathbf{Q}'\mathbf{K}'^\top + \gamma \mathbf{K}'\beta^\top + \gamma \mathbf{Q}'\beta^\top + \beta^2}{\sqrt{D_k}}\right).$$

Thus, we have established the equivalence stated in Eq. 1, demonstrating how the normalized attention mechanism relates to the original formulation through a series of algebraic transformations. \square